**BAJOPMAS JOURNAL 16(1): 65 – 80**
Printed in Bayero University, Kano - Nigeria.

# DECIPHERMENT OF THE SUBSURFACE USING ELECTRICAL GEOPHYSICAL METHOD FOR BOREHOLE OPTIMIZATION, A CASE STUDY AT HOTORO KUDU, NASSARAWA LOCAL GOVERNMENT, KANO STATE

**Ibrahim, H. S., Saleh, M., Lawan, M. S., Shehu, Y.**
Department of Physics, Aliko Dangote University of Science and Technology, Wudil
Department of Physics, Bayero University, Kano, Nigeria

## ABSTRACT

This study applied Direct Current Resistivity, Induced Polarization (IP), and Self-Potential (SP) geophysical methods to evaluate the aquifer characteristics in Hotoro Kudu, Nassarawa Local Government Area, Kano, Nigeria. The study area covers approximately 5 km² and lies between latitudes 11.96001°N and 11.98005°N, and longitudes 8.57002°E and 8.59000°E. The acquired geophysical datasets were subjected to reduction, processing, and interpretation, which enabled the delineation of prospective zones for groundwater exploration.The identified groundwater targets are situated between latitudes 11.96700°N and 11.97000°N with longitudes 8.58600°E to 8.58820°E, as well as latitude 11.97100°N and longitude 8.58850°E. The estimated aquifer depth within these zones ranges from 100 m to 130 m. The very low IP values suggest the presence of unconsolidated sediments characterized by appreciable porosity and permeability, indicating a high recharge potential and, therefore, a sustainable groundwater resource. Furthermore, the observed range of SP values reflects variations in groundwater flow, indicating upward and downward movement through porous and/or fractured formations.Subsurface characterization revealed six distinct lithological units: Sandy Soil with Clay, Clayey Sandy Soil, Clay, Weathered Basement, Fractured Basement, and Fresh Basement Complex rocks. Based on the integrated geophysical interpretation, a drilling depth of approximately 140 m is recommended for groundwater development within the delineated zones.



**Key words:** Anthropogenic, Aquifer, Electrical, Geophysical, Indices, Spontaneous

## 1.0 INTRODUCTION

The inadequacy of water affects the human chain and other organisms. To satisfy the demand of water, people are relying more on aquifers [1]. Aquifers are geological formations that store groundwater within porous materials or permeable rocks, provided they possess sufficient storage capacity and hydraulic conductivity [2]. The development and characteristics of aquifers are governed by several factors, including past geomorphological processes, the depositional environment during rock formation, the mineralogical composition of the aquifer materials, the mechanisms and patterns of groundwater flow, and the residence time of groundwater within the host formations [2].The occurrence and distribution of groundwater within these zones are further controlled by parameters such as the nature of the parent rock, the depth, extent, and pattern of weathering, the thickness of the weathered overburden, the sand-to-clay ratio, and the degree of fracturing, fissuring, and jointing within the bedrock [1]. At present, the proper characterization of bedrock aquifers and their sustainable development is fundamental to achieving short-term water security [3].Since aquifer units are not directly observable at the surface, identifying potential groundwater resources requires subsurface investigation to delineate aquifer-bearing layers.

These aquifers vary spatially in terms of depth and thickness; in some locations, they are difficult to detect, whereas in others, they are relatively easy to identify [2].

Geo-electrical resistivity survey is amongst the geophysical technology frequently used in the exploration for groundwater for its simplicity in field application, fluctuating adjustable depth of investigation giving useful information about layers being investigated including their level of saturation [4], availability of robust 1D, 2D, and 3D interpretation software in both porous and fissured media [5]. The technique has been established and has become a fundamental instrument in hydrological studies, hydrogeological prospecting etc [6].The basic principle that describe the measurement of subsurface distinction with the use of geo-electrical resistivity below the earth was propounded by Schlumberger who implemented the earliest experiment in the year 1912. Field techniques have evolved significantly, transitioning from manual measurements conducted at isolated and independent points to the use of programmed systems hiring multi-electrode arrays arranged along a measurement profile. Consequently, fast, mechanized multi-electrode and multichannel data acquisition systems are now available, offering greater flexibility in the acquisition of geo-electrical resistivity data [6]. This method has wide applications in hydrogeological studies, including the appraisal of aquifer depth and thickness, detection of contaminant plumes, determination of aquifer hydraulic properties, monitoring of aquifer recharge, and classification of saline intrusion in coastal aquifers [5]. The technique has also been successfully applied in numerous groundwater exploration campaigns [4], [5].



In the search for an aquifer, groundwater assessment, modeling, well design and construction especially for areas requiring such useful information, there is the need to properly measure and interpret hydrological features, this thrusts the use of geo-electrical resistivity method for this research, essentially to localize an aquifer and its estimated depth of investigation in the study area which is essential in the search of groundwater and also to map out the stratigraphy of the study area. Hotoro Kudu at Nassarawa Local government area, Kano State is among the cities with large population and besieged to get adequate water for daily activities [1].

### 1.2 Location and Geology of the Study Area

The study area, Hotoro Kudu Nassarawa Local Government, Kano State, Nigeria is located along Maiduguri Road, opposite to the Abubakar Rimi Television Broadcasting Station. The area is bounded between the latitude $11.753888^0$N to $11.759423^0$N and longitudes $8.275286^0$E to $8.287099^0$E. Figure1 is a map showing the boundary of the study area. In the study area, groundwater occurs within the weathered mantle or in the joint and fracture systems of the unweathered or partly weathered rocks [7]. [7] Proposed that, aquifers are found within the weathered mantle and fractured rock, where permeability and penetrability are enough to permit considerable amounts of water to accumulate in storage. High groundwater yield in the area is observed where thick overburden overlies fractured zones. The aquifer types identified in the study area include the weathered layer aquifer, the weathered/fractured (or partly weathered) aquifer, and the fractured aquifer [7]**.** Kano state including the study area experiences a tropical climate having a rainy and a dry season. Rainy season begins in April/May and ends in October while dry season prevails for the rest

of the year. [7]. The least humidity value is recorded between January and February, and the highest, between July and September [8].

Apart from annual precipitation, there is no proximate surface water resource to recharge the aquifers in the study area. Therefore, rainfall is considered the major source of recharging aquifers in the area. Due to the absence of surface and tap water supplied by the water authorities, there is no other alternate than to exploit groundwater to meet all water requirements of the area.

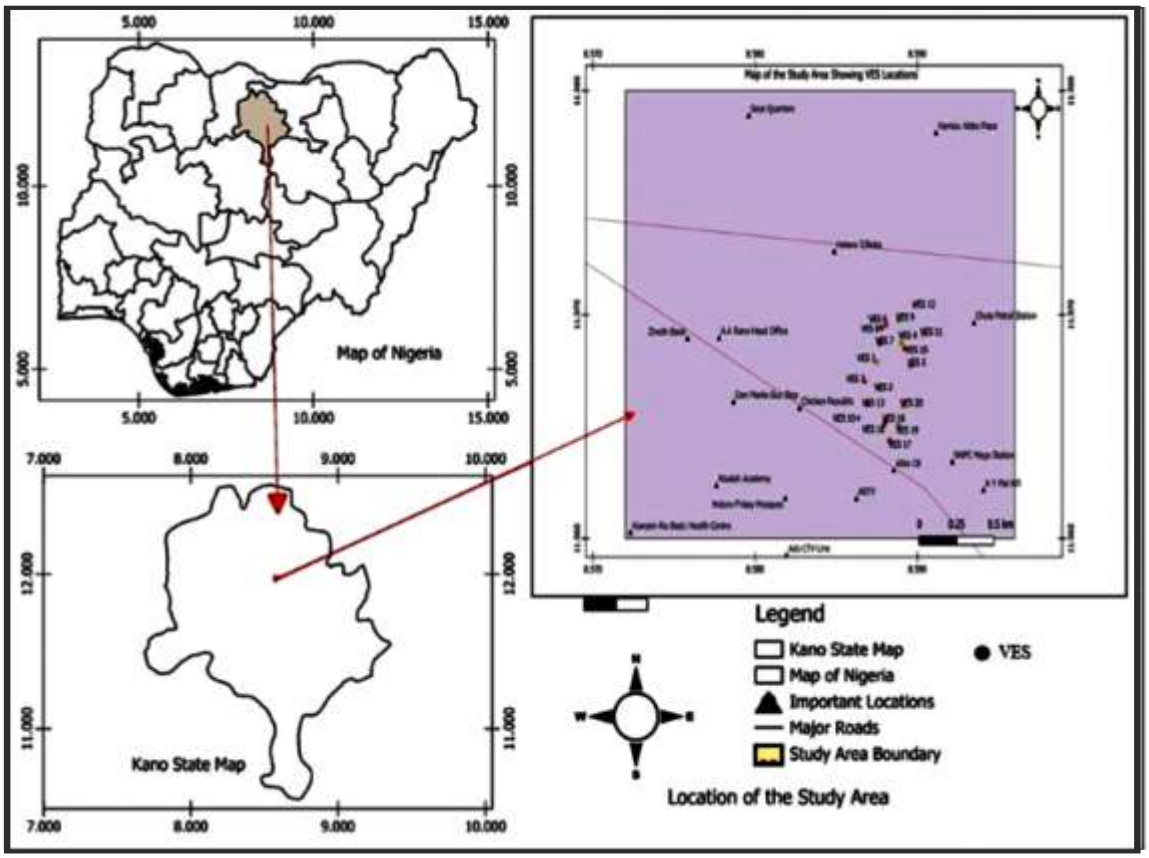


**Figure 1: Map of the Study Area Showing All the VES Stations [9]**

## 2.0 MATERIALS AND METHODS

### 2.1 Materials

The following are the materials used in data acquisition:

i. ABEM signal averaging system (SAS) 1000 Terrameter
ii. 12 V car battery
iii. Stainless steel electrodes
iv. Connecting wires
v. Hammers
vi. Measuring Tape
vii. GPS
viii. Solar Panel
ix. Sample bottles

## 2.2 Method

The resistivity method is employed in this work. The method employs an artificial source of current which is introduced into the ground through point electrodes or long wire contacts. The procedure is to measure potentials at other electrodes in the vicinity of the current flow. Electrical methods of geophysical investigations are based on the resistivity or its inverse, that is; conductivity of materials. The electrical resistance, R of a material is related to its physical dimension, cross sectional area, A, length, L, through the resistivity ρ by [1]

$$\rho = \frac{RA}{L} \quad (1)$$

However, [10] asserted that, the resistivity $\rho$ is further related to the apparent resistivity $R_{app}$ and geometric factor K as;

$$\rho = R_{app} K \quad (2)$$

In addition, [11] has shown that for four electrodes system, the schlumberger array geometric factor (K) is given by;

$$K_{schlumberger} = \frac{\pi}{MN}\left[\frac{AB}{2}\right]^2 \quad [3]$$

Furthermore, under the resistivity method, the Vertical Electrical Sounding (electrical drilling 1D) using Schlumberger array was adopted. In the schlumberger array, four electrodes are placed symmetrically along a straight line, the potential electrodes on the inside while the current electrodes on the outside (Figure 2).



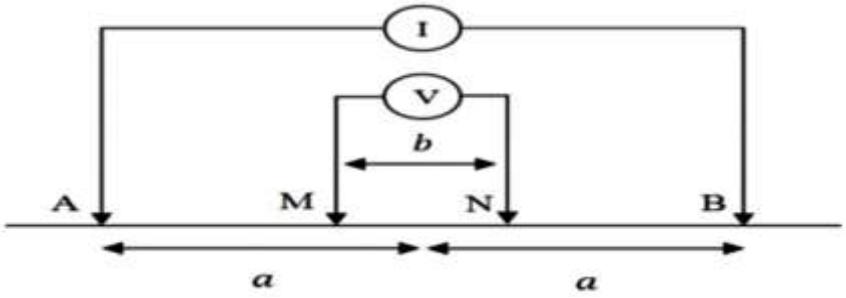


**Figure 2 Schlumberger configuration array [12]**

This configuration consists of a pair of current and potential electrodes. These electrodes are driven into the ground in a straight line to make good contact with the earth. The current electrode spacing is expanded over a range of values for measurements in the field and this significantly changes the range of measurements and its corresponding depth of investigations. However, as the measurement progresses, the current electrodes (AB/2) separation increases gradually to a far distance apart while the potential electrodes (MN/2) are kept at small separations relative to the current electrodes separations (Table 1) as a result, the method required less labor and financial commitment and this is one of the major advantages of this method over other methods [6]. Nevertheless, when the ratio of the distance between the current electrodes to that between the potential electrodes becomes too large, the potential electrodes must also be displaced outwards otherwise the potential difference becomes too small to be measured with sufficient accuracy [6].

**Table 1 VES No 19, Hotoro Kudu, U/Mahauta Gayawa street**
**VES No19. Lat:11.9650501$^0$N Long: 8.5888351$^0$E**

| S/N | AB/2 (M) | MN/2 (M) | RES (ΩM) | IP (Ms) | SP (Mv) |
|---|---|---|---|---|---|
| 1 | 1.50 | 0.50 | 36.97 | 14.50 | -21.82 |
| 2 | 2.00 | 0.50 | 33.05 | -0.87 | -21.05 |
| 3 | 3.00 | 0.50 | 28.94 | -75.80 | -19.90 |
| 4 | 4.50 | 0.50 | 70.82 K | -670.00 | -19.38 |
| 5 | 7.00 | 0.50 | 38.57 | 78.20 | -18.87 |
| 6 | 10.0 | 0.50 | 31.52 | -134.00 | -18.25 |
| 7 | 10.0 | 2.00 | 36.41 | -41.80 | -0.23 |
| 8 | 12.0 | 2.00 | 50.77 | -19.00 | -0.17 |
| 9 | 15.0 | 2.00 | 103.00 | 3.30 | -0.17 |
| 10 | 17.0 | 2.00 | 24.87 | -289.00 | -0.16 |
| 11 | 20.0 | 2.00 | 77.95 K | -506.00 | -0.16 |
| 12 | 25.0 | 2.00 | 28.16 | -104.00 | -0.16 |
| 13 | 30.0 | 2.00 | 29.37 | -3.54 | -94.81 |
| 14 | 45.0 | 10.00 | 79.41 | -1.84 | -53.39 |
| 15 | 60.0 | 10.00 | 96.17 | -9.13 | -30.57 |
| 16 | 70.0 | 10.00 | -10.49 | -156.00 | -9.59 |
| 17 | 80.0 | 10.00 | 106.63 | -13.10 | 1.17 |
| 18 | 100.0 | 10.00 | 146.52 | -10.50 | 7.20 |
| 19 | 120.0 | 10.00 | 159.05 | -20.80 | 13.16 |
| 20 | 150.0 | 10.00 | 124.58 | -107.00 | 19.00 |
| 21 | 170.0 | 10.00 | 234.05 | -20.70 | 26.98 |
| 22 | 200.0 | 10.00 | -125.78 | 305.00 | 27.59 |



During the field work of taking sounding readings, the terrameter performs automatic recording of resistivity, induced polarization and self-potential values (Table 1) and digitally displays it in real time [6]. However, during the field work of data acquisition, twenty Vertical Electrical Sounding (20 VES) points were recorded. IPI2WIN software aided in the interpretation of all the VES raw data. In addition, Microsoft excels and Surfer 11 softwares were used and processed the IP and SP data respectively thereby, generating contour maps which were crucial in the interpretation of the geological data obtained.

## 3.0 RESULTS AND DISCUSSION

The resistivity data acquired (Table 1) for the twenty VES station was processed using IPI2WIN software. The resistivity values were plotted against the electrode distance (AB/2)

about each profile of all the VES stations. The software processed two windows i.e. the Model Parameter Tables Window and Curves Window as shown on figure 3 and 4 respectively. Nineteen more of its kind were collected, processed and developed into twenty parameter tables and their corresponding curve windows (with respect to their VES stations) using the IPI2Win software.

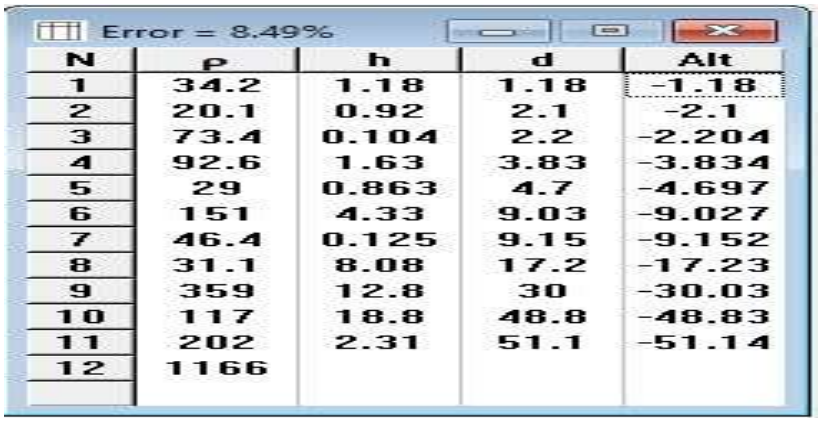


| N | ρ | h | d | Alt |
|---|---|---|---|---|
| 1 | 34.2 | 1.18 | 1.18 | -1.18 |
| 2 | 20.1 | 0.92 | 2.1 | -2.1 |
| 3 | 73.4 | 0.104 | 2.2 | -2.204 |
| 4 | 92.6 | 1.63 | 3.83 | -3.834 |
| 5 | 29 | 0.863 | 4.7 | -4.697 |
| 6 | 151 | 4.33 | 9.03 | -9.027 |
| 7 | 46.4 | 0.125 | 9.15 | -9.152 |
| 8 | 31.1 | 8.08 | 17.2 | -17.23 |
| 9 | 359 | 12.8 | 30 | -30.03 |
| 10 | 117 | 18.8 | 48.8 | -48.83 |
| 11 | 202 | 2.31 | 51.1 | -51.14 |
| 12 | 1166 | | | |

**Figure 3. VES 19: Apparent Resistivity Model Parameter Windows**



In figure 3, the resistivity model parameter window comprises of five columns. The column headers designated N (number of layer), ρ {apparent resistivity (Ωm)} which decodes the resistivity values of each layer, h {layer thickness (m)}, d {depth to the bottom of layer (m)} and the alt {altitude (m)} [13].

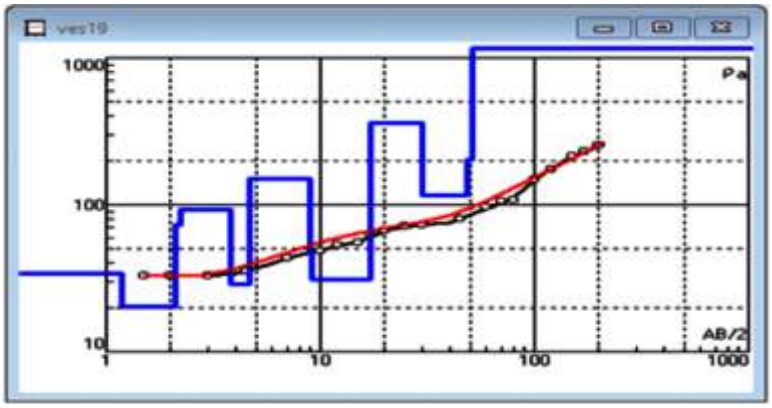


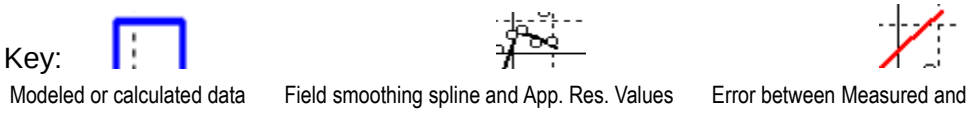


**Figure 4. VES 19: Apparent Resistivity Curve Windows using the IPI2WIN software.**

On the other hand, the curve parameter window (Figure 4) also a representative sample of the apparent resistivity curve window which is composed of four superimposed curves. The curve itself is presented by a black line which is a smoothing spline on the field values and the circles along the black line are the field values of apparent resistivity. The blue line represents the modeled or calculated data, such as the theoretical apparent resistivity curve based on the inversion result. However, the red line represents the error or difference between the measured and calculated data [13].

### 3.1 Stratigraphy of the Study Area

The model parameter tables for each VES stations were used in categorizing the stratigraphy and locating the depths of favorable groundwater accumulation of the study area.

With the aid of the advanced parameter table window (Figure 3) the result was validated using the borehole log of the study area (Table 2) and yielded the stratigraphy of all the twenty VES stations (Table 3).

**Table 2. Borehole Log and Resistivity Ranges for Kano State Weathering Grades [5]**

| Material | Resistivity-range(Ωm) |
|---|---|
| Sandy soil with clay | 60 – 100 |
| Clayey sandy soil | 30 – 60 |
| Clay | 10 – 50 |
| Weathered basement | 50 – 150 |
| Fractured basement | 150 – 400 |
| Fresh basement | 750 – 8000 |



**Table 3. Sample stratigraphy of VES 19 station**

| Layer | Res (Ωm) | Depth (m) | Material |
|---|---|---|---|
| (i) | 92.60 | 3.83 | Sandy soil with clay |
| (ii) | 151.0 | 9.03 | Weathered basement |
| (iii) | 31.10 | 17.2 | Clay |
| (iv) | 359.0 | 30.0 | Fractured basement |
| (v) | 117.0 | 48.8 | Weathered basement |

The processed data have shown that, a maximum of six geological layers above the fresh basement complex rock namely; clayey soil with clay, clay, weathered basement, fractured basement, sandy soil with clay and fresh basement were delineated in the study area (Table 3), similar stratigraphy was reported by [14].

Out of all the 20 VES stations, one station, VES 16 (Lat: 11.9652650N Long: 8.5880350E) was found to have six layers, another five stations; VES 5 (Lat: 11.96771170N Long: 8.58591$^0$E), VES 7 (Lat: 11.96873170E Long: 8.58770170N), VES 12 (Lat: 11.9704150N Long: 8.5898317$^0$E), VES 18 (Lat: 11.96512$^0$N Long: 8.5879717$^0$E) and VES 19 (Lat:11.9650501$^0$N) Long: 8.5888351$^0$E) are with five geological layers. Moreover, six more stations VES 1 (Lat: 11.9678749$^0$N Long: 8.5874871$^0$E), VES 3 (Lat: 11.9670336$^0$N Long: 8.5867632$^0$E), VES 8 (Lat: 11.969420$^0$N Long: 8.58780$^0$E), VES 9 (Lat: 11.9697615$^0$N Long: 8.5888339$^0$E), VES 10 (Lat: 11.9687417$^0$N Long: 8.589020E) and VES 13 (Lat: 11.9659967$^0$N Long: 8.5869417$^0$E) found with four different layers. In addition, eight more stations VES 2 (Lat: 11.96670$^0$N Long: 8.587700$^0$E), VES 4 (Lat: 11.9776123$^0$N Long: 8.57481$^0$E), VES 6 (Lat: 11.9766118$^0$N Long: 8.59482$^0$E), VES 11 (Lat: 11.96908$^0$N Long: 8.5903617$^0$E) VES 14 (Lat: 11.9659967$^0$N Long: 8.5869417$^0$E), VES 15 (Lat:11.96538$^0$N Long: 8.58636$^0$E), VES 17 (Lat: 11.9643667$^0$N Long: 8.5882883$^0$E) and VES 20 (Lat: 11.9659232$^0$N Long: 8.5891379$^0$E) found with three geological layers.

These lithology-layers contribute to the development of groundwater because it serves as the passage for the movement of surface water to the fractured layers. The topsoil generally consists of three parts: the belt of soil water at the top, the intermediate vadose zone and the capillary fringe at the bottom [6].

### 3.2 Suitable Locations for Groundwater Explorations and Their Estimated Depth

The Microsoft excel software was used and processed the IP and SP data. A plot of IP and SP values against the depths of investigation at each VES station were made, thereby portraying the graphical features of the highest depths values each of IP and SP (Figure 4)

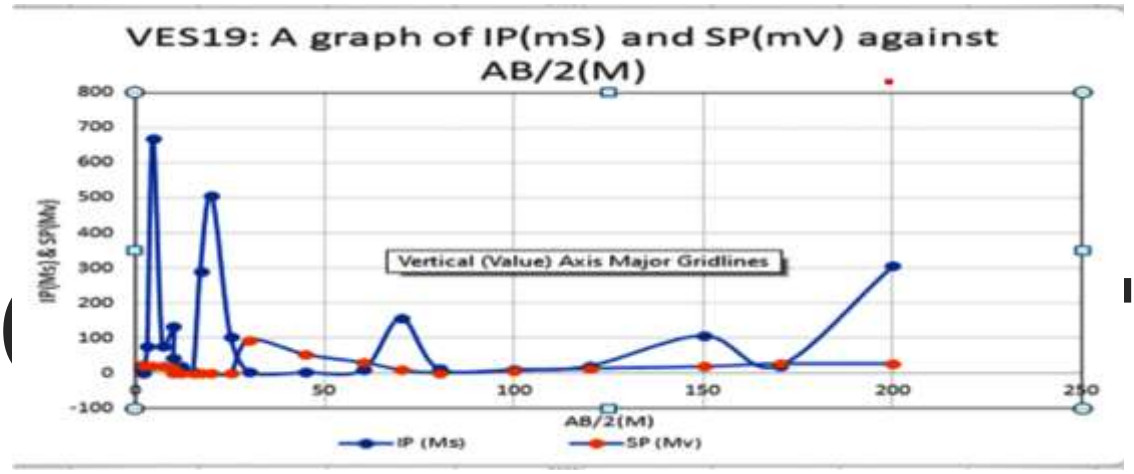


**Figure 5.A sample plot of IP (mS) and SP (mV) against the depth of investigation for VES 19 using the Microsoft excel software.**

The typical graph sample plot is presented on (Figure 4). The blue dots represents chargeability values of the subsurface materials (IP (mS) ) which indicates the ability of the materials present in the subsurface to hold an electric charge, at specific depth, higher IP values suggests the presence of permeable layer [14]. The red dots on the other hand, it symbolizes SP (mV) values and signifies a natural voltage difference in the subsurface and often influenced by electrochemical reactions indicating the existence of groundwater flow at higher values [8].

Coupled with the coordinates of all the VES points, the highest depth value each of resistivity, IP and SP that is not above the fresh basement were recorded and inputted into the surfer 11 software, thereby generating three different basement topography Contour Maps of Resistivity depth, IP depth and SP depth at specific coordinates; Figures 5, 6 and 7 represents the maps respectively.

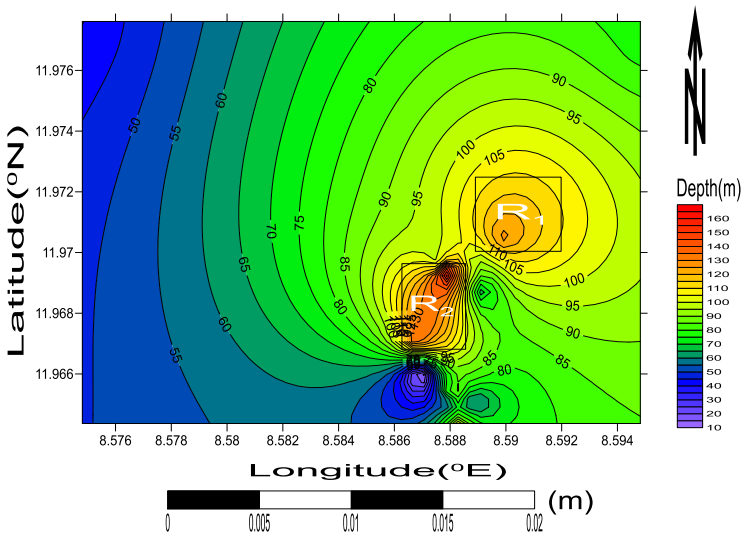


**Figure 5 Fresh Basement Rocks Topography Based on Resistivity Data using the Surfer 11 software.**

Figure 5 shows the range of resistivity and the estimated depth of investigation values obtained as; 350-650 (Ωm) at 110 m and 100-300 (Ωm) at 130 m for $R_1$ and $R_2$ respectively.



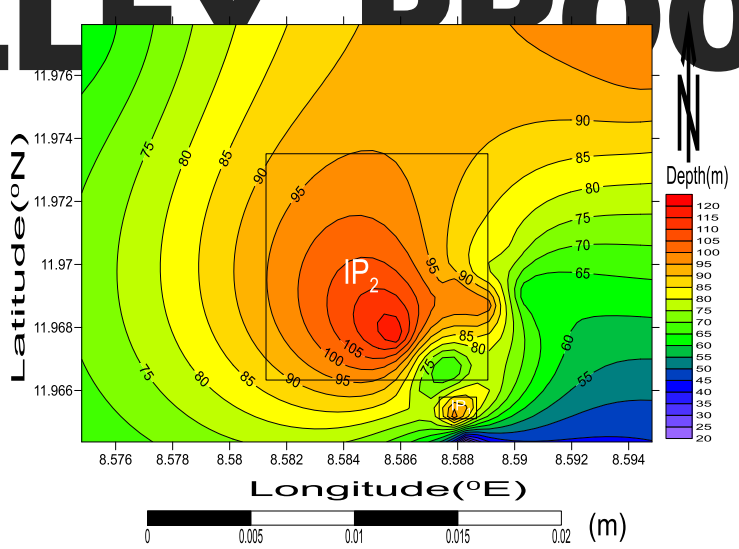


**Figure 6 Fresh Basement Rocks Topography Based on IP Data using the Surfer 11 software.**

However, in the contour map of IP (Figure 6), IP values and their estimated depth of investigations at particular coordinates were delineated as; 45–150 mS at 110m and 10–40 mS at 90 m for $IP_1$ and $IP_2$ respectively.

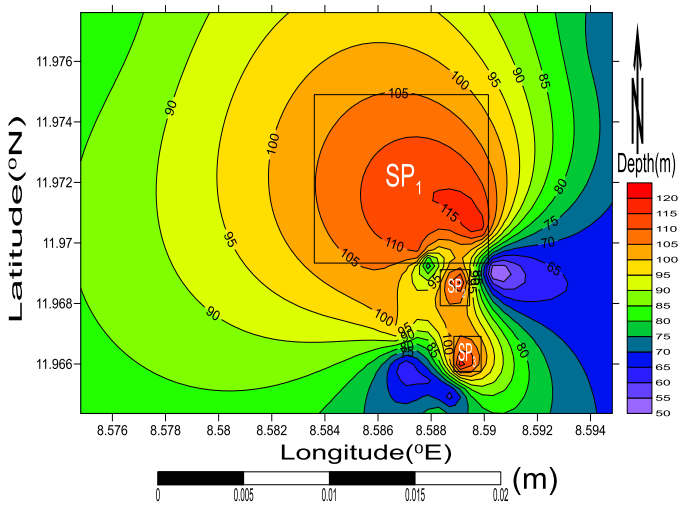


**Figure 7 Fresh Basement Rocks Topography Based on SP Data using the Surfer 11 software.**

In addition, figure 7 represents the contour map of the SP values and their expected depth of investigations at specific coordinates. Their distinguished values are; 30–44 mV at 120m, 45–65 mV at 110 m and 70–100 mV at 105 m for the $SP_1$, $SP_2$ and $SP_3$ respectively.



**Table 4 A table showing the maximum depth recorded at specific Coordinates (Lat,Long) for Resistivity, IP and SP respectively using Surfer 11 software.**

| S/N | Parameter | Lat (°N) | | Long (°E) | | Depth (m) |
|---|---|---|---|---|---|---|
| | | Start | End | Start | End | |
| 1 | $R_1$ | 8.59147 | 8.59161 | 11.9701 | 11.9723 | 110 |
| 2 | $R_2$ | 8.58839 | 8.5885 | 11.6707 | 11.9695 | 130 |
| 3 | $IP_1$ | 8.58847 | 8.58859 | 11.9649 | 11.9659 | 90 |
| 4 | $IP_2$ | 8.58707 | 8.86968 | 11.9669 | 11.9716 | 110 |
| 5 | $SP_1$ | 8.58999 | 8.59016 | 11.9698 | 11.9734 | 120 |
| 6 | $SP_2$ | 8.5896 | 8.58971 | 11.9679 | 11.9688 | 110 |
| 7 | $SP_3$ | 8.59022 | 8.5887 | 11.9657 | 11.6665 | 105 |

Table 4 serves as the grand summary for the estimated depth of investigation at specific coordinates (which is vital in the result interpretation) for all the parameters (resistivity, IP and SP) measured in this research.

**Table 5 Typical Chargeability Values adopted for this Research [5]**

| Rock Type | Chargeability (mS) |
|---|---|
| Alluvium | 0 - 5 |
| Latetrite/Quarzilite Rocks | 6 - 25 |
| Weathered Basement Complex Rocks | 26 – 54 |
| Fractured Basement Complex Rocks | 55 - 70 |
| Fresh Basement Complex Rocks | 71 and above |

Based on the presence and combination of the parameters measured (Resistivity, IP and SP) at specific coordinates, a strategic focus on promising zones of groundwater prospective of a specific location, two locations were identified namely; Point I and Point II. The point identification offers a clear background for interpreting the geophysical data and planning subsequent exploration or development activities.

**Point i**

When the depth of all the three categories of geophysical parameters; resistivity, IP and SP (e.g., $R_1IP_1SP_2$ or $R_2IP_2SP_3$ or $R_1IP_1SP_2$ and etc.) is detected at deeper position and in the same coordinate, such location is classified 'Most Favorable Location' and are highly anticipated to be the most promising zone for groundwater potential.

**Point ii**

When the depth of any two of the three parameters measured such as resistivity, and any of IP or SP (e.g., $R_2SP_3$ or $R_1IP_2$ and etc.) is discovered at a deeper point and within the same coordinate, such positions are categorized as 'Good Locations' for groundwater. This indicates a strong likelihood of groundwater being present, though not as certain as in the "Position I" category as such, further surveys or investigations are required to confirm the findings.

### 3.3 Cross Correlation and Geological Interpretation of Point I ($R_2IP_2SP_3$)



Three out of the three parameters mapped out by contour maps were overlapped at the range of 100-130m depth (Table 4). They overlapped between the latitude 11.96700 $^0$N to 11.97000 $^0$N and longitudes 8.58600 $^0$E to 8.58820 $^0$E. Within the depth of investigation, the resistivity value ranges between (50 – 3490 Ωm). At higher resistivity values typically >300 Ωm indicates the consolidated gravel or fractured rock formation (Table 2). At moderate resistivity >150 Ωm fractured rocks with higher water content is expected and at lower resistivity range typically <150 Ωm weathered rocks with lower water content is expected, (Table 2). However, within depth of investigation, the IP ranges between (0-40mS). IP values at lower range (<10 mS) suggests the presence of Alluvium (Table 5) while at the higher range of values of IP (≤40 mS) indicates the presence of Weathered basement rock (Table 5). Additionally, the range of SP values (70 –110 mS) at this depth indicates electrochemical reactions suggesting the groundwater flow.

*Groundwater potential of point I*

The depth range of 'Point I' location (100-130 m) (Table 4) and the resistivity values suggests the presence of clayey sandy soil and consolidated or fractured rock formation. The overall range of resistivity values (50-349 Ωm) suggested moderate and high conductivity, which indicates an 'Aquifer' particularly due to the presence of high water with significant clay content at lower resistance range (water may not be clean). The groundwater bearing zones in the area is mostly located between the clay and the sand clay layer corresponding to fourth layer. The responsible factor for this is attributed to porosity and permeability of aquifer contents. Clay has high porosity; hence, half of its volume store water. The void between clay particles is microscopically small with large surface area favors slow movement and retention of water. Clays do not make good aquifers compared to sand clay with lower porosity for free flow of water as sands clays have more interconnected pores. While the high resistivity range (≥150 Ωm) at 100-130m depth indicates porous or fractured rock formations hosting a 'Confined Aquifer' According to [15]**,** a successful well is

often predicted to be developed in the sandstone formation when the resistivity is, between (150 -600) Ωm, whereas an unproductive well may result if the bedrock resistivity is over 800 Ωm**.** The high resistivity may be attributed to due to freshwater which has not been contaminated with the leachate from the dumpsite [5].

On the other hand, the presence of Alluvium rock due to very low IP value indicates the occurrence of unconsolidated sediments such as silt, sand and gravel which has permeability and porosity, consequently, alluvium rock can recharge quickly making it a promising and sustainable source of groundwater This result is in agreement with [15] who indicated that, low chargeability values (< 7.0 mS) give a supportive interpretation of water containing zone for this area, he further asserted that, in the water zone, the low values of chargeability are reflected in a water-saturated zone as water is a poor medium to retain electrical charges. The chargeability values for IP indicate gravel, sandstone or alluvium**.** Not only that, higher IP values (closer to 40 mS) suggest the presence of weathered basement materials and likely clays or fine sediments which suggests the existence of 'Confine Aquifer' at 100 m. Additionally, the overall range of SP value (30-65 mV) at a maximum depth if 120 m indicates the rise and fall of groundwater flow through porous or fractured zone from more active movement at higher SP range of values and relatively moderate low at lower SP range of values [17] reported that, one of the mechanisms producing SP is electrokinetic potential which is observed when a fluid is forced through a capillary or porous medium. This effect is shown in Equation (2.7). It is evident from this equation that the electric potential $E_k$ is dependent on the pressure gradient $\Delta p$. Hence points with high SP values with great depths indicate higher flow. The consequential information of the research findings shows that, all 'Point I' category is graded 'Excellent location" for groundwater prospection.



### 3.4 Cross Correlation and Geological Interpretation of Point II

Two out of the three parameters recorded by the contour maps within the study area matched between the depth ranges of 100 – 130m (Table 4).They covered the area between the Lat 11.97100 $^0$N to 11.9710 $^0$N and Lon 8.5885 $^0$E to 8.5885 $^0$E. Within the depth of investigation, the resistivity values ranges between (350 – 650 Ωm). The intermediate resistivity range of (350-650Ωm) indicates the presence of fractured basement (Table 2). However, the value of SP within the depth of investigation is at the range of (30–44mV) suggesting the natural electrochemical potentials generated by groundwater movement in porous or fractured formations.

*Groundwater Potential of 'Point II'*

The depth and resistivity range of $R_1SP_1$ of (100-130) m and (350-650) Ωm respectively suggests a likely potential 'Deeper Aquifer' in porous or fractured formations and sandy rock layer saturated with groundwater. However, the typically high resistivity range (350-650) Ωm at deeper depth of 110 m suggests the potential existence of a clean, freshwater and protected aquifer, particularly in fractured rock formations. Not only that, the high SP value at a depth of 105 m strongly indicates the presence of active groundwater flow suggesting a productive. This is also consistent with similar studies conducted by [17]. In addition, the SP values (at higher SP range) and at a depth of 110 m indicates the presence of groundwater

flow especially within fractured formations, [17] indicates a dominancy of positive SP peaks with value ranging from 80 to 120 mV. The resulting evidence of the study outcomes indicates that, 'Point II' class is rated 'valuable location" for groundwater exploration.

## 4.0 CONCLUSION

Investigation of groundwater potential in Hotoro Kudu, Nassarawa Local government area Kano State has been carried out through the use of Vertical Electrical Sounding (VES). The result of the twenty VES carried out revealed that; there are six geological layers; sandy soil with clay, clayey sandy soil, clay, weathered basement, fractured basement, and fresh basement in the study area. However out of the twenty VES stations, one station (VES 16) was found to have six geological layers; five stations (VES 5, 7, 12, 18, and 19) enclosed five layers; six more stations (VES 1, 3, 8, 9, 10, and 13) had four layers; furthermore, eight other stations (VES 2, 4, 6, 11, 14, 15, 17, and 20) were found to have three geological layers. It was essentially observed that, within the study area, there are three levels of aquifer viz ; highly productive aquifer at the depth of 130 m, moderately-yield aquifer at the depth of 110m and low-yield aquifer at the depth of 100 m where steady and sustainable borehole could be dug.



## REFERENCES

[1] M. Umar, A. Y. Abubakar & M. A. Aliyu (2019) Geoelectric Investigation of Potential Underground Borehole Sites in Some Part of Nassarawa Local Government Area of Kano State, Nigeria. Dutse Journal of Pure and Applied Sciences (DUJOPAS), Vol. 5 No. 2b

[2] Aswar Syafnur, Haidir Jibran, William Desmond Tonapa, Ashar Sae and Nur Hidayat Nurdin (2023). Investigation of Groundwater Aquifer Using Electrical Resistivity Method Wenner-Schlumberger Array Mattoangin Village, Bantimurung District, Maros Regency. Jurnal Geocelebes Vol. 7 No. 1, ISSN: 2579-5821 (Print) ISSN: 2579-5546 (Online) URL address: http://journal.unhas.ac.id/index.php/geocelebes DOI: 10.20956/geocelebes.v7i1.23302

[3] Wahab, S., Saibi H. & Mizunaga, H. (2021). Groundwater aquifer detection using the electrical resistivity method at Ito Campus, Kyushu University (Fukuoka, Japan). Geoscience Letters, 8, 15. https://doi.org/10.1186/s40562-021-00188-6.

[4] Aweda, A.K., Jatau, B.S. and Goki, N.G. (2023) Groundwater Investigation Using Electrical Resistivity Method at the Edati Hill, Northern Bida Basin, Nigeria. British Journal of Multidisciplinary and Advanced Studies: Sciences, 4(2),23-35, 2023 Print ISSN: 2517-276X Online ISSN: 2517-2778 Website: https://bjmas.org/index.php/bjmas/index

[5] Reynolds, J. M. R. (2011). *An Introduction to Applied and Environmental Geophysics* (Second Edi, Issue 606). John Wiley.

[6] Joel E.S., Oyanameh O.E, Fatoye O.V., Ayeni J.K & Sunday,R.M (2022). Investigation of groundwater potential in Atan-Ota, Ogun State, South-western Nigeria. Vol. 2 No 2,

[7] M. Umar, A. Y. Abubakar & M. A. Aliyu (2019) Geoelectric Investigation of Potential Underground Borehole Sites in Some Part of Nassarawa Local Government Area of

Kano State, Nigeria. Dutse Journal of Pure and Applied Sciences (DUJOPAS), Vol. 5 No. 2b

[8] *Government Area of Kano State Nigeria*. *3*(1), 1–6. https://doi.org/10.9790/0990-03110106 Yelwa, N. A., Hamidu, H., Falalu, B. H., Kana, M. A., & Madabo, I. M. (2015). *Groundwater prospecting and Aquifer Delineation using Vertical Electrical Sounding ( VES ) method in the Basement complex terrain of Kumbotso Local*

[9] Abubakar Yusuf Ismail & Auwal Lawal Yola (2012) Geoelectrical Investigation of Groundwater Potential of Dawakin Tofa Local Government Area of Kano State Nigeria. American International Journal of Contemporary Research Vol. 2

[10] Tahir A. G, Garba and Girie M. B (2014). Subsurface Lithology and Aquifer Zones Using Vertical Electrical Sounding Method in Kano Metropolis, Northwestern Nigeria. IOSR Journal of Applied Geology and Geophysics (IOSR-JAGG) e-ISSN: 2321–0990, p-ISSN: 2321–0982.Volume 2, Issue 6 Ver. II, PP 46-51 www.iosrjournals.org

[11] Tri Rahajoeningroem and Bagus Indrajana (2020) Groundwater Potential Investigation Using Geoelectric Method with Schlumberger Electrode Configuration in Catur Rahayu Village, Dendang District. IOP Conf. Series: Materials Science and Engineering 879 (2020) 012115 IOP Publishing doi:10.1088/1757-899X/879/1/012115



[12] Jannatul Hasni Omar1, Nordila Ahmad, Jestn Jelani, Zuliziana Suif1 and Maidiana Othman (2023) Geophysical Investigation of Groundwater Resources Using Electrical Resistivity and Induced Polarization Method. International Journal of GEOMATE, Vol. 25, Issue 107, pp.235-242 ISSN: 2186-2982 (P), 2186-2990 (O), Japan, DOI: https://doi.org/10.21660/2023.107.s8510

[13] User's Guide (2002) IPI2Win (MT) (Second version, Department of Geophysics, Moscow State University.

[14] Kumar, R., Tiwari, A. K., Yadav, G.S. and Singh, N. P. (2014). Geohydrological Investigation using vertical Electrical Sounding at Banaras Hindu University Campus, Varansi, U. P India. International Journal of Research in Engineering and Technology. Vol. 3: pp. 252-256.

[15] Omar, J. H., Ahmad, N., Jelani, J., Suif, Z., & Othman, M. (2023). *Geophysical investigation of groundwater resources using electrical resistivity and induced polarization method*. *25*(107), 235–242.

[16] R. Bello, G. O. Emujakporue, U. U. M. and B. G. G. (2017). *The use of vertical electrical sounding (ves) to investigate the extent of groundwater contamination and lithology delineation at a dumpsite in aluu community, rivers state. 16*(1), 182–191.

[17] Jamaluddeen, S. S., Bunawa, A. A., & Saleh, M. (2014). *An Assessment of the Groundwater Potential of Bayero University Kano Permanent Site Using Induced Polarization and Self-potential Methods*. *4*, 587–596. https://doi.org/10.17265/2159-581X/2014.10.001

[18] Aizebeokhai, A. P., Oyeyemi, K., & Joel, E. S. (2016). *Electrical resistivity and induced-polarization imaging for groundwater exploration*. *September*. https://doi.org/10.1190/segam2016-13857737.1

## APPENDICES

| N | ρ | h | d | Alt |
|---|---|---|---|---|
| 1 | 64.7 | 0.112 | 0.112 | -0.112 |
| 2 | 41.8 | 0.144 | 0.256 | -0.256 |
| 3 | 22.1 | 0.144 | 0.4 | -0.4 |
| 4 | 5.2 | 1.01 | 1.41 | -1.41 |
| 5 | 35.8 | 0.0445 | 1.45 | -1.454 |
| 6 | 103 | 1.01 | 2.46 | -2.464 |
| 7 | 103 | 9.59 | 12.1 | -12.05 |
| 8 | 37.5 | 1.07 | 13.1 | -13.12 |
| 9 | 44.2 | 7.86 | 21 | -20.98 |
| 10 | 73 | 4.46 | 25.4 | -25.44 |
| 11 | 167 | 0.795 | 26.2 | -26.24 |
| 12 | 279 | 41.4 | 67.6 | -67.64 |
| 13 | 1000 | | | |

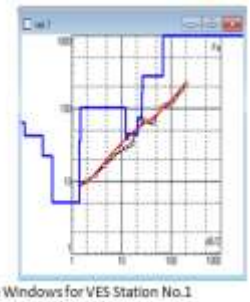

Apparent Resistivity Model Parameter Table and Curve Windows for VES Station No.1

| N | ρ | h | d | Alt |
|---|---|---|---|---|
| 1 | 13.7 | 0.804 | 0.804 | -0.804 |
| 2 | 41.6 | 0.302 | 1.11 | -1.106 |
| 3 | 20.3 | 1.34 | 2.45 | -2.445 |
| 4 | 34.2 | 0.648 | 3.09 | -3.094 |
| 5 | 251 | 0.943 | 4.04 | -4.037 |
| 6 | 139 | 3.37 | 7.41 | -7.407 |
| 7 | 124 | 2.61 | 10 | -10.02 |
| 8 | 50.2 | 8.68 | 18.7 | -18.7 |
| 9 | 106 | 0.26 | 19 | -18.96 |
| 10 | 293 | 11.9 | 30.9 | -30.86 |
| 11 | 388 | 75.6 | 106 | -106.5 |
| 12 | 1166 | | | |

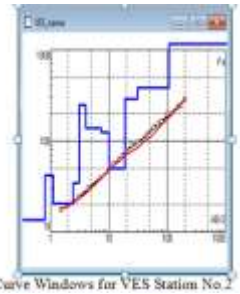

Apparent Resistivity Model Parameter Table and Curve Windows for VES Station No.2

| N | ρ | h | d | Alt |
|---|---|---|---|---|
| 1 | 29.7 | 0.0715 | 0.0715 | -0.0715 |
| 2 | 2.31 | 0.213 | 0.285 | -0.2845 |
| 3 | 28.5 | 0.49 | 0.775 | -0.7745 |
| 4 | 74.6 | 0.251 | 1.03 | -1.026 |
| 5 | 45.9 | 3.11 | 4.14 | -4.135 |
| 6 | 48.9 | 2.28 | 6.42 | -6.415 |
| 7 | 66.7 | 4.95 | 11.4 | -11.37 |
| 8 | 137 | 9.1 | 20.5 | -20.47 |
| 9 | 113 | 0.346 | 20.8 | -20.81 |
| 10 | 186 | 0.733 | 21.5 | -21.54 |
| 11 | 264 | 46.6 | 68.1 | -68.14 |
| 12 | 514 | 71.3 | 139 | -139.4 |
| 13 | 1227 | | | |

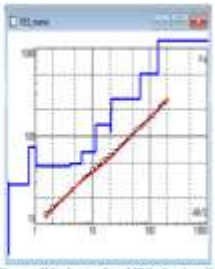

Apparent Resistivity Model Parameter Table and Curve Windows for VES Station No.3

| N | ρ | h | d | Alt |
|---|---|---|---|---|
| 1 | 47.1 | 0.885 | 0.885 | -0.885 |
| 2 | 20.2 | 0.494 | 1.38 | -1.379 |
| 3 | 97.5 | 0.888 | 2.27 | -2.267 |
| 4 | 21 | 1.3 | 3.57 | -3.567 |
| 5 | 34.8 | 1.29 | 4.86 | -4.857 |
| 6 | 298 | 1.42 | 6.28 | -6.277 |
| 7 | 441 | 16.4 | 22.7 | -22.68 |
| 8 | 359 | 3.76 | 26.4 | -26.44 |
| 9 | 215 | 1.04 | 27.5 | -27.48 |
| 10 | 291 | 12 | 39.5 | -39.48 |
| 11 | 378 | 0.295 | 39.8 | -39.77 |
| 12 | 5812 | | | |

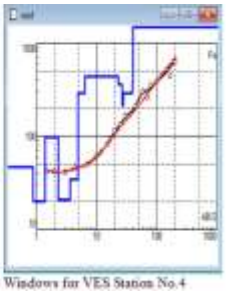

Apparent Resistivity Model Parameter Table and Curve Windows for VES Station No.4

| N | ρ | h | d | Alt |
|---|---|---|---|---|
| 1 | 47.1 | 0.664 | 0.664 | -0.664 |
| 2 | 38.8 | 0.715 | 1.38 | -1.379 |
| 3 | 97.5 | 0.888 | 2.27 | -2.267 |
| 4 | 35.9 | 1.24 | 3.51 | -3.587 |
| 5 | 34.8 | 0.478 | 3.98 | -3.985 |
| 6 | 143 | 5.05 | 9.03 | -9.035 |
| 7 | 41.9 | 9.44 | 18.5 | -18.47 |
| 8 | 359 | 7.92 | 26.4 | -26.39 |
| 9 | 388 | 5.23 | 31.6 | -31.62 |
| 10 | 251 | 7.81 | 39.4 | -39.43 |
| 11 | 90.3 | 60.6 | 100 | -100 |
| 12 | 858 | | | |

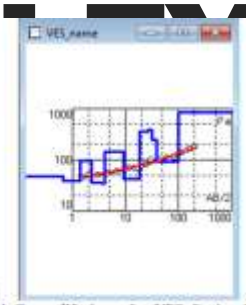

Apparent Resistivity Model Parameter Table and Curve Windows for VES Station No.5

| N | ρ | h | d | Alt |
|---|---|---|---|---|
| 1 | 35.3 | 0.82 | 0.82 | -0.82 |
| 2 | 26.4 | 0.511 | 1.33 | -1.331 |
| 3 | 69.9 | 0.352 | 1.68 | -1.683 |
| 4 | 233 | 1.35 | 3.03 | -3.033 |
| 5 | 215 | 1.13 | 4.16 | -4.163 |
| 6 | 233 | 1.25 | 5.41 | -5.413 |
| 7 | 233 | 1.94 | 7.35 | -7.353 |
| 8 | 285 | 7.7 | 15.1 | -15.05 |
| 9 | 239 | 10.1 | 25.2 | -25.15 |
| 10 | 388 | 11.8 | 37 | -36.95 |
| 11 | 264 | 40.6 | 77.6 | -77.55 |
| 12 | 1053 | | | |

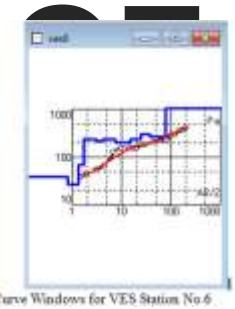

Apparent Resistivity Model Parameter Table and Curve Windows for VES Station No.6

| N | ρ | h | d | Alt |
|---|---|---|---|---|
| 1 | 35 | 0.9 | 0.9 | -0.9 |
| 2 | 198 | 0.481 | 1.38 | -1.381 |
| 3 | 198 | 0.738 | 2.12 | -2.119 |
| 4 | 67.3 | 1.13 | 3.25 | -3.249 |
| 5 | 44.8 | 1.74 | 4.99 | -4.989 |
| 6 | 81.8 | 2.67 | 7.66 | -7.659 |
| 7 | 191 | 4.09 | 11.7 | -11.75 |
| 8 | 68.5 | 6.28 | 18 | -18.03 |
| 9 | 116 | 9.64 | 27.7 | -27.67 |
| 10 | 245 | 14.8 | 42.5 | -42.47 |
| 11 | 295 | 14.5 | 57 | -56.97 |
| 12 | 75.5 | 43 | 100 | -99.97 |
| 13 | 1259 | | | |

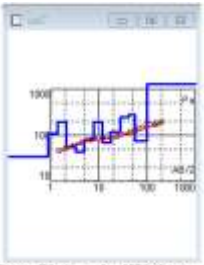

Apparent Resistivity Model Parameter Table and Curve Windows for VES Station No.7

| N | ρ | h | d | Alt |
|---|---|---|---|---|
| 1 | 30 | 0.9 | 0.9 | -0.9 |
| 2 | 52.8 | 0.481 | 1.38 | -1.381 |
| 3 | 215 | 0.738 | 2.12 | -2.119 |
| 4 | 233 | 1.13 | 3.25 | -3.249 |
| 5 | 156 | 1.74 | 4.99 | -4.989 |
| 6 | 38.8 | 6.76 | 11.7 | -11.75 |
| 7 | 388 | 6.28 | 18 | -18.03 |
| 8 | 324 | 13.6 | 31.6 | -31.63 |
| 9 | 67.5 | 10.8 | 42.4 | -42.43 |
| 10 | 102 | 25.7 | 68.1 | -68.13 |
| 11 | 359 | 107 | 175 | -175.1 |
| 12 | 1227 | | | |

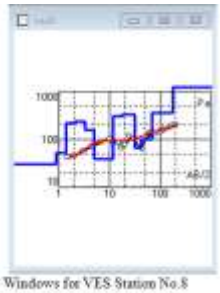

Apparent Resistivity Model Parameter Table and Curve Windows for VES Station No.8

| N | ρ | h | d | Alt |
|---|---|---|---|---|
| 1 | 36.9 | 0.669 | 0.669 | -0.669 |
| 2 | 158 | 0.244 | 0.913 | -0.913 |
| 3 | 37.8 | 1.06 | 1.97 | -1.973 |
| 4 | 26.9 | 0.965 | 2.94 | -2.938 |
| 5 | 258 | 0.0666 | 3 | -3.005 |
| 6 | 258 | 3.8 | 6.8 | -6.805 |
| 7 | 48.1 | 7.76 | 14.6 | -14.56 |
| 8 | 203 | 23 | 37.6 | -37.56 |
| 9 | 29.7 | 3.66 | 41.2 | -41.22 |
| 10 | 66.1 | 35.8 | 77 | -77.02 |
| 11 | 255 | 17.2 | 94.2 | -94.22 |
| 12 | 1586 | | | |

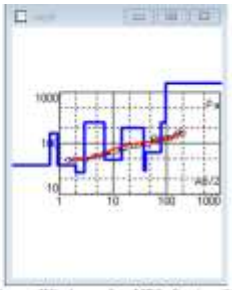

Apparent Resistivity Model Parameter Table and Curve Windows for VES Station No.9

| N | ρ | h | d | Alt |
|---|---|---|---|---|
| 1 | 13.7 | 0.786 | 0.786 | -0.786 |
| 2 | 341 | 0.682 | 1.47 | -1.468 |
| 3 | 245 | 0.527 | 1.99 | -1.995 |
| 4 | 278 | 0.838 | 2.83 | -2.834 |
| 5 | 67.2 | 2.05 | 4.88 | -4.884 |
| 6 | 78.4 | 2.69 | 7.57 | -7.574 |
| 7 | 151 | 3.41 | 11 | -10.98 |
| 8 | 227 | 4.61 | 15.6 | -15.59 |
| 9 | 209 | 11 | 26.6 | -26.59 |
| 10 | 221 | 16.8 | 43.4 | -43.39 |
| 11 | 528 | 21.8 | 65.2 | -65.19 |
| 12 | 1395 | | | |

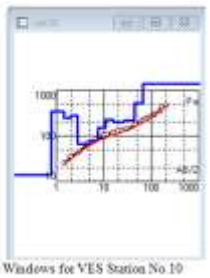

Apparent Resistivity Model Parameter Table and Curve Windows for VES Station No.10

| N | ρ | h | d | Alt |
|---|---|---|---|---|
| 1 | 9.71 | 0.913 | 0.913 | -0.913 |
| 2 | 63.1 | 0.374 | 1.29 | -1.287 |
| 3 | 185 | 0.775 | 2.06 | -2.062 |
| 4 | 71.9 | 1.36 | 3.42 | -3.422 |
| 5 | 370 | 1.01 | 4.43 | -4.432 |
| 6 | 324 | 2.94 | 7.37 | -7.372 |
| 7 | 233 | 3.12 | 10.5 | -10.49 |
| 8 | 84 | 7.16 | 17.7 | -17.65 |
| 9 | 370 | 6.59 | 24.2 | -24.24 |
| 10 | 489 | 38.2 | 62.4 | -62.44 |
| 11 | 238 | 37.6 | 100 | -100 |
| 12 | 1196 | | | |

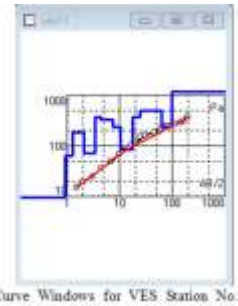

Apparent Resistivity Model Parameter Table and Curve Windows for VES Station No.11

| N | ρ | h | d | Alt |
|---|---|---|---|---|
| 1 | 45.8 | 0.723 | 0.723 | -0.723 |
| 2 | 180 | 0.318 | 1.04 | -1.041 |
| 3 | 32.4 | 1.02 | 2.06 | -2.061 |
| 4 | 128 | 0.902 | 2.96 | -2.963 |
| 5 | 1032 | 1.97 | 4.93 | -4.933 |
| 6 | 365 | 1.64 | 6.57 | -6.573 |
| 7 | 48.3 | 5.61 | 12.2 | -12.18 |
| 8 | 142 | 3.69 | 15.9 | -15.87 |
| 9 | 2411 | 10.7 | 26.6 | -26.57 |
| 10 | 1284 | 9.47 | 36 | -36.04 |
| 11 | 76.8 | 49.1 | 85.1 | -85.14 |
| 12 | 7115 | | | |

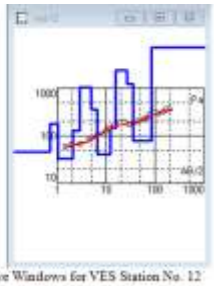

Apparent Resistivity Model Parameter Table and Curve Windows for VES Station No. 12

| N | ρ | h | d | Alt |
|---|---|---|---|---|
| 1 | 513 | 0.9 | 0.9 | -0.9 |
| 2 | 489 | 0.481 | 1.38 | -1.381 |
| 3 | 1545 | 0.738 | 2.12 | -2.119 |
| 4 | 1755 | 1.13 | 3.25 | -3.249 |
| 5 | 1245 | 1.74 | 4.99 | -4.989 |
| 6 | 5552 | 4.51 | 9.5 | -9.489 |
| 7 | 4338 | 1.3 | 10.8 | -10.8 |
| 8 | 2754 | 7.24 | 18 | -18.04 |
| 9 | 2288 | 9.64 | 27.7 | -27.68 |
| 10 | 2636 | 14.8 | 42.5 | -42.48 |
| 11 | 5183 | 22.7 | 65.2 | -65.18 |
| 12 | 4542 | 34.8 | 100 | -99.98 |
| 13 | 4946 | | | |

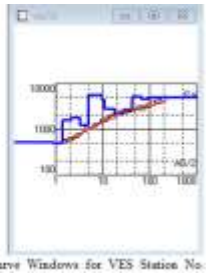

Apparent Resistivity Model Parameter Table and Curve Windows for VES Station No. 13

| N | ρ | h | d | Alt |
|---|---|---|---|---|
| 1 | 47.2 | 0.639 | 0.639 | -0.639 |
| 2 | 200 | 0.28 | 0.919 | -0.919 |
| 3 | 58.3 | 0.994 | 1.91 | -1.913 |
| 4 | 250 | 0.747 | 2.66 | -2.66 |
| 5 | 574 | 3.99 | 6.65 | -6.65 |
| 6 | 201 | 0.162 | 6.81 | -6.812 |
| 7 | 293 | 7.73 | 14.5 | -14.54 |
| 8 | 441 | 13 | 27.5 | -27.54 |
| 9 | 483 | 3.32 | 30.9 | -30.86 |
| 10 | 158 | 31.8 | 62.7 | -62.66 |
| 11 | 356 | 19.5 | 82.2 | -82.16 |
| 12 | 1431 | | | |

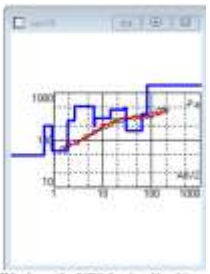

Apparent Resistivity Model Parameter Table and Curve Windows for VES Station No. 14

| N | ρ | h | d | Alt |
|---|---|---|---|---|
| 1 | 40.8 | 0.793 | 0.793 | -0.793 |
| 2 | 185 | 0.752 | 1.54 | -1.545 |
| 3 | 73.6 | 0.705 | 2.25 | -2.25 |
| 4 | 88.3 | 0.575 | 2.83 | -2.825 |
| 5 | 359 | 1.84 | 4.66 | -4.665 |
| 6 | 273 | 1.56 | 6.22 | -6.225 |
| 7 | 112 | 3.53 | 9.76 | -9.755 |
| 8 | 293 | 6.35 | 16.1 | -16.1 |
| 9 | 333 | 10.7 | 26.8 | -26.81 |
| 10 | 369 | 12 | 38.8 | -38.81 |
| 11 | 391 | 1.01 | 39.8 | -39.81 |
| 12 | 1227 | | | |

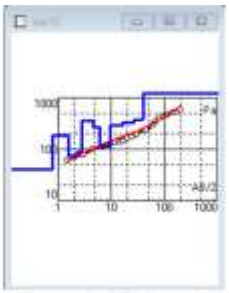

Apparent Resistivity Model Parameter Table and Curve Windows for VES Station No. 15

| N | ρ | h | d | Alt |
|---|---|---|---|---|
| 1 | 16.6 | 0.476 | 0.476 | -0.476 |
| 2 | 52.8 | 0.45 | 0.926 | -0.926 |
| 3 | 47.6 | 1.17 | 2.1 | -2.096 |
| 4 | 145 | 0.786 | 2.8 | -2.882 |
| 5 | 295 | 1.75 | 4.55 | -4.552 |
| 6 | 167 | 2.72 | 7.27 | -7.272 |
| 7 | 398 | 3.18 | 10.5 | -10.45 |
| 8 | 89.9 | 7.19 | 17.6 | -17.64 |
| 9 | 445 | 6.21 | 23.9 | -23.85 |
| 10 | 324 | 44.2 | 68.1 | -68.05 |
| 11 | 431 | 28.6 | 96.7 | -96.65 |
| 12 | 1468 | | | |

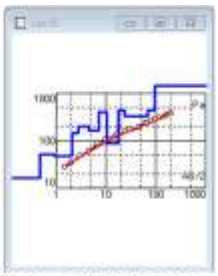

Apparent Resistivity Model Parameter Table and Curve Windows for VES Station No. 16

| N | ρ | h | d | Alt |
|---|---|---|---|---|
| 1 | 35 | 0.9 | 0.9 | -0.9 |
| 2 | 55.5 | 0.481 | 1.38 | -1.381 |
| 3 | 69.6 | 0.738 | 2.12 | -2.119 |
| 4 | 126 | 1.13 | 3.25 | -3.249 |
| 5 | 187 | 2.3 | 5.55 | -5.549 |
| 6 | 464 | 2.19 | 7.74 | -7.739 |
| 7 | 420 | 4.01 | 11.7 | -11.75 |
| 8 | 221 | 5.81 | 17.6 | -17.56 |
| 9 | 373 | 10.1 | 27.7 | -27.66 |
| 10 | 369 | 14.8 | 42.5 | -42.46 |
| 11 | 570 | 22.7 | 65.2 | -65.16 |
| 12 | 569 | 34.8 | 100 | -99.96 |
| 13 | 1359 | | | |

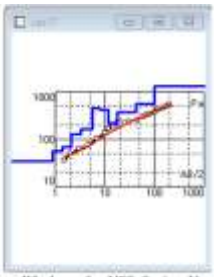

Apparent Resistivity Model Parameter Table and Curve Windows for VES Station No. 17

| N | ρ | h | d | Alt |
|---|---|---|---|---|
| 1 | 31.1 | 0.828 | 0.828 | -0.828 |
| 2 | 137 | 0.461 | 1.29 | -1.289 |
| 3 | 49.8 | 0.793 | 2.08 | -2.082 |
| 4 | 127 | 1.17 | 3.25 | -3.252 |
| 5 | 132 | 2.03 | 5.28 | -5.282 |
| 6 | 38 | 4.31 | 9.59 | -9.592 |
| 7 | 48.6 | 6.25 | 15.8 | -15.84 |
| 8 | 275 | 4.94 | 20.8 | -20.78 |
| 9 | 53.8 | 3.42 | 24.2 | -24.2 |
| 10 | 105 | 18.5 | 42.7 | -42.7 |
| 11 | 35.4 | 9.46 | 52.2 | -52.16 |
| 12 | 1359 | | | |

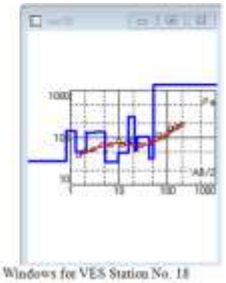

Apparent Resistivity Model Parameter Table and Curve Windows for VES Station No. 18

| N | ρ | h | d | Alt |
|---|---|---|---|---|
| 1 | 34.2 | 1.18 | 1.18 | -1.18 |
| 2 | 20.1 | 0.92 | 2.1 | -2.1 |
| 3 | 73.4 | 0.104 | 2.2 | -2.204 |
| 4 | 92.6 | 1.63 | 3.83 | -3.834 |
| 5 | 28 | 0.863 | 4.7 | -4.697 |
| 6 | 151 | 4.33 | 9.03 | -9.027 |
| 7 | 46.4 | 0.125 | 9.15 | -9.152 |
| 8 | 31.1 | 8.08 | 17.2 | -17.23 |
| 9 | 359 | 12.8 | 30 | -30.03 |
| 10 | 117 | 18.8 | 48.8 | -48.83 |
| 11 | 202 | 2.31 | 51.1 | -51.14 |
| 12 | 1166 | | | |

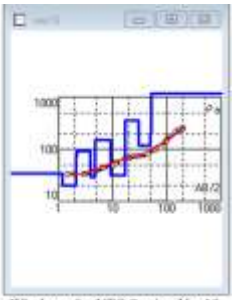

Apparent Resistivity Model Parameter Table and Curve Windows for VES Station No. 19

| N | ρ | h | d | Alt |
|---|---|---|---|---|
| 1 | 528 | 0.456 | 0.456 | -0.456 |
| 2 | 239 | 1.06 | 1.52 | -1.516 |
| 3 | 341 | 1.64 | 3.16 | -3.156 |
| 4 | 233 | 0.928 | 4.08 | -4.084 |
| 5 | 555 | 4.06 | 8.14 | -8.144 |
| 6 | 251 | 2.27 | 10.4 | -10.41 |
| 7 | 489 | 4.77 | 15.2 | -15.18 |
| 8 | 452 | 12.5 | 27.7 | -27.68 |
| 9 | 514 | 37.1 | 64.8 | -64.78 |
| 10 | 686 | 16.4 | 81.2 | -81.18 |
| 11 | 1545 | 118 | 199 | -199.2 |
| 12 | 1431 | | | |

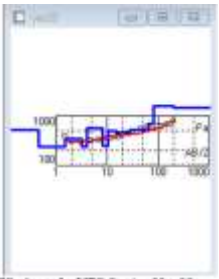

Apparent Resistivity Model Parameter Table and Curve Windows for VES Station No. 20